40th Conference on Radar Meteorology

Poster #157

Impact of Assimilating Retrieval Thermodynamic Fields and Radar Data

*Chieh-Ying Ke[a], Kao-Shen Chung[a], Yu-Chieng Liou[a], Chih-Chien Tsai[b]

[a] Department of Atmospheric Sciences, National Central University, Taiwan

[b] National Science and Technology Center for Disaster Reduction, New Taipei City, Taiwan

Email : cyke812@g.ncu.edu.tw

ABSTRACT

To investigate the potential benefits of assimilating 3D temperature and water-vapor information in addition to radar observations in multiscale weather systems, a thermodynamics retrieval algorithm was employed, and three sets of observing system simulation experiments (OSSEs) were conducted by using the WRF–LETKF Radar Assimilation System (WLRAS). With one frontal system accompanied heavy rainfall case study, results showed that assimilating temperature data had a significant impact on the final analysis at the mid-level of stratiform areas despite the warm and wet bias of the retrieved elds, resulting in improved forecasts of heavy rainfall. On the other hand, assimilating water vapor information only helped to reconstruct the range and intensity of the cold pool near the surface, but the improvement in 3-hour rainfall forecast was limited. The optimal results of analysis and short-term forecast were achieved when both the retrieved temperature and water vapor were assimilated. Overall, this study illustrated the benefits of assimilating three-dimensional thermal variables in multiscale precipitation systems.

Terrain-Permitting Thermodynamic Retrieval Scheme (TPTRS) And Moisture adjustment method

The thermodynamic retrieval starts with the momentum equations:

$$F \equiv -\frac{1}{\theta_{v0}}\left[\frac{\partial u}{\partial t} + \vec{V}\cdot\nabla u - fv + turb(u)\right] = -\frac{\partial \pi'}{\partial x} \qquad (1)$$

$$G \equiv -\frac{1}{\theta_{v0}}\left[\frac{\partial v}{\partial t} + \vec{V}\cdot\nabla v + fu + turb(v)\right] = -\frac{\partial \pi'}{\partial y} \qquad (2)$$

$$H \equiv -\frac{1}{\theta_{v0}}\left[\frac{\partial w}{\partial t} + \vec{V}\cdot\nabla w + turb(w) + g(q_r)\right] = -\frac{\partial \pi'}{\partial z} + g\frac{\theta'_c}{\theta_{v0}\theta_0} \qquad (3)$$

$$u\frac{\partial \theta'_c}{\partial x} + v\frac{\partial \theta'_c}{\partial y} + w\frac{\partial \theta'_c}{\partial z} + w\frac{\partial \theta_0}{\partial z} + S = 0 \qquad (4)$$

The F, G, and H can be obtained once the 3-D air motion is obtained through multiple-Doppler-radar synthesis. The terrain-permitting thermodynamic retrieval scheme is an algorithm for immediately retrieving the 3D pressure and temperature fields for complex terrain using wind information.

The moisture adjustment method was based on that of Liou et al. (2014), who proposed a simple and effective approach for adjusting temperature and moisture fields through iterative methods. When the radar reflectivity exceeds 10 dBZ, this area is regarded as saturated.

OSSEs : Assimilating Retrieved Thermodynamic Variables

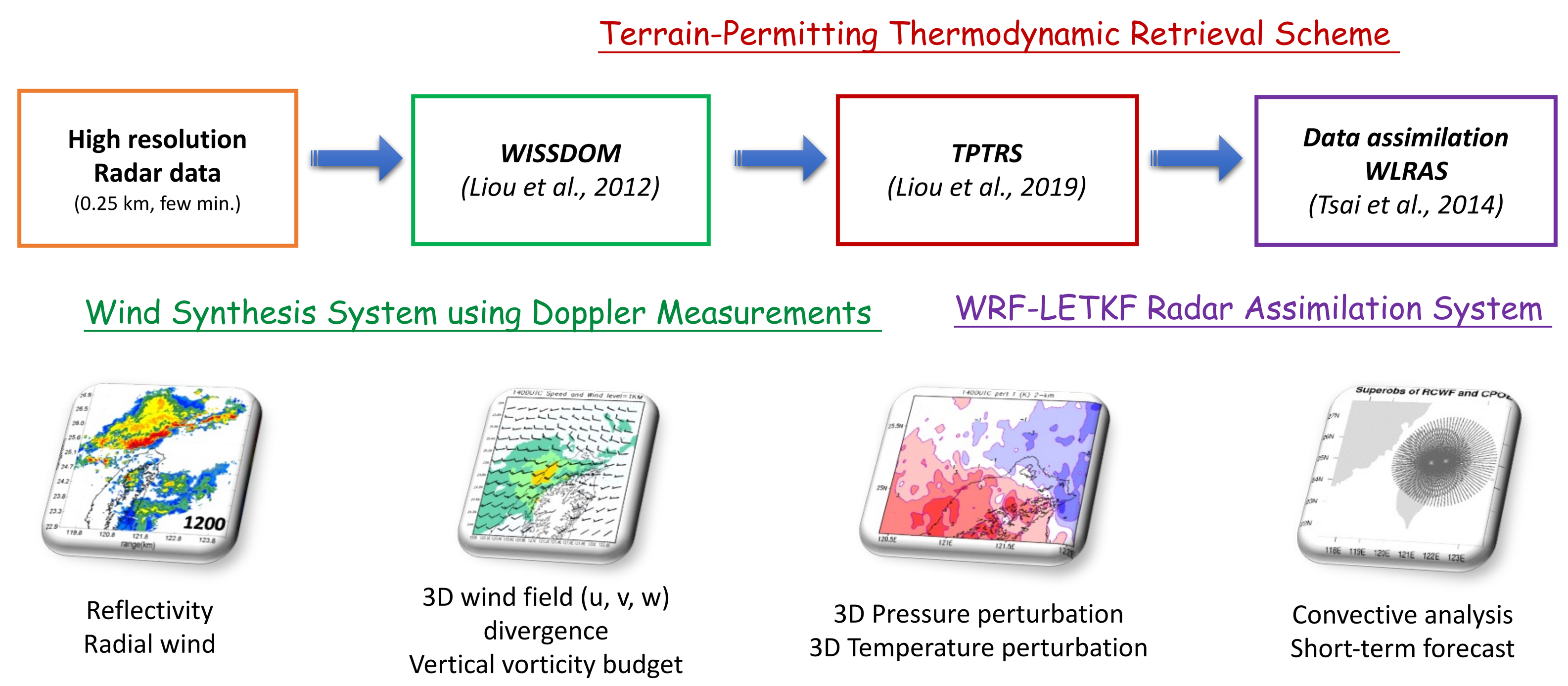

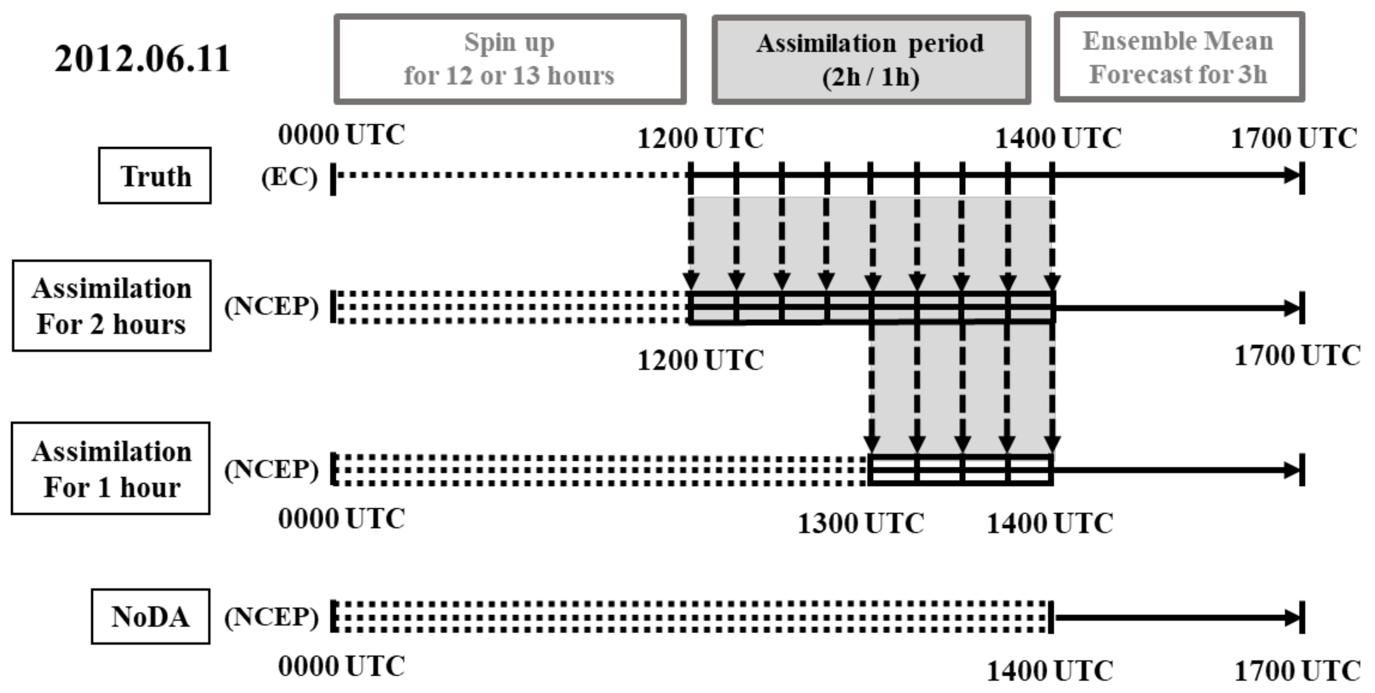

OSSE experiments Truth and NoDA

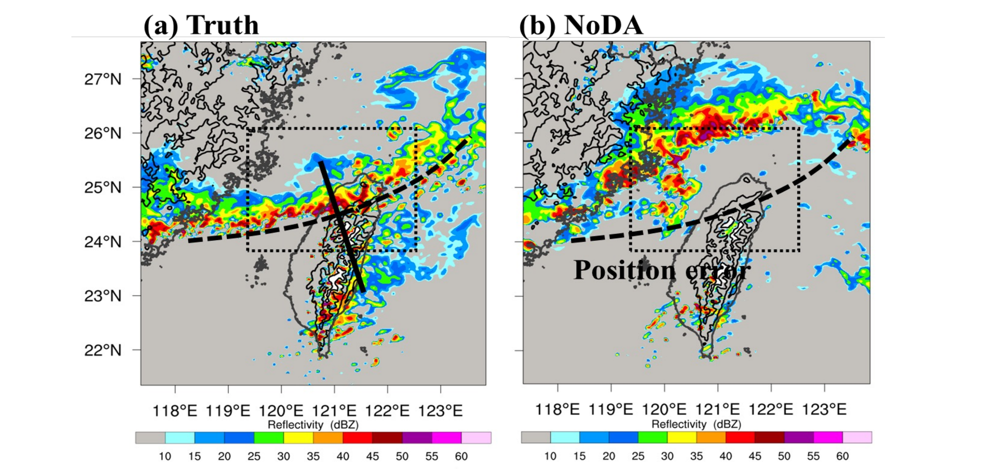

Fig. 1. Simulation of reflectivity at 1400 UTC

Retrieval Thermodynamic Variables

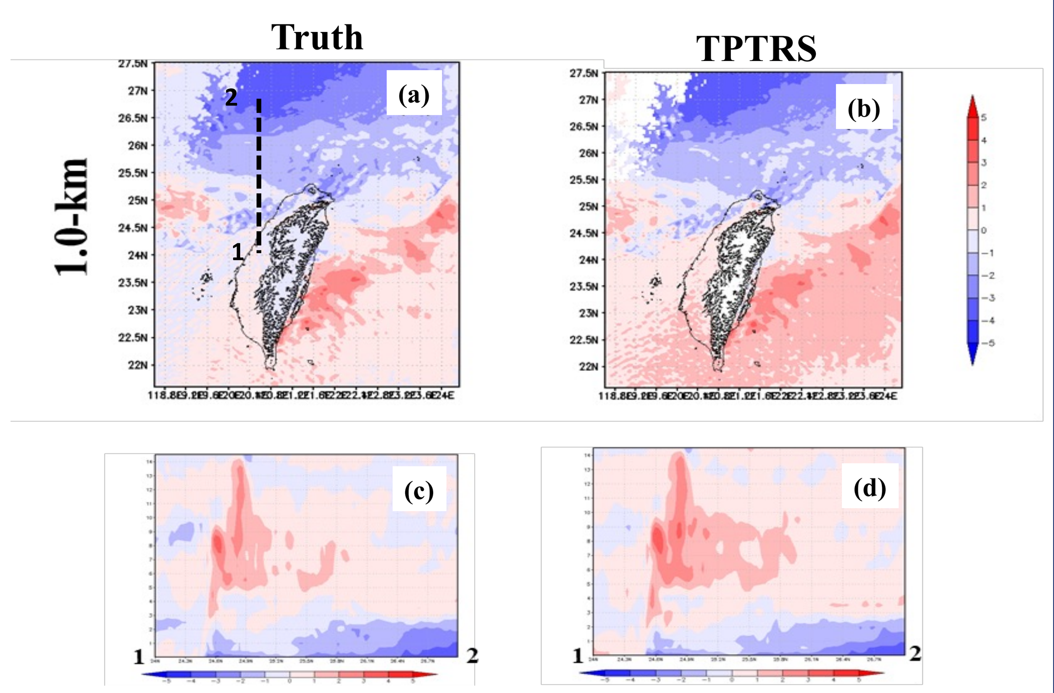

Fig. 2. Temperature perturbation from Truth and Retrieved from TPTRS. Cross-section along line 1-2.

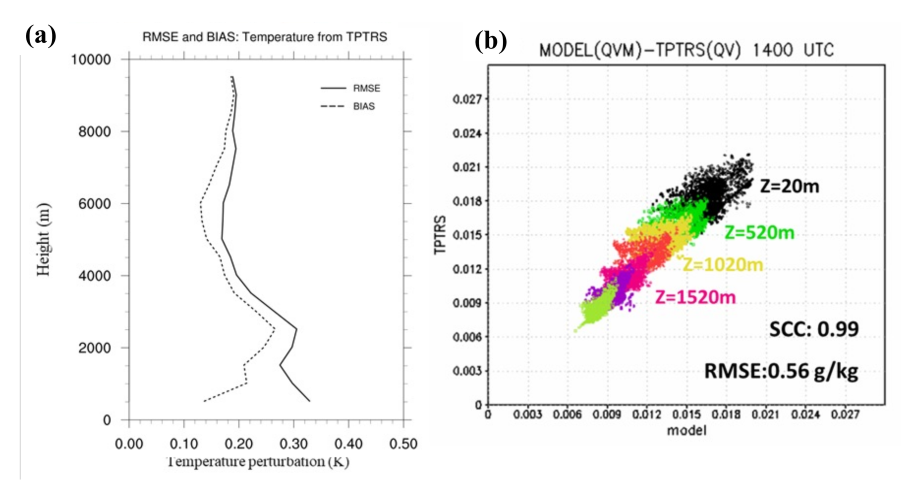

Fig. 3. (a) Vertical profile of retrieval temperature RMSE and BIAS. (b) Scatter plot of water vapor between truth model and retrieved by TPTRS.

Results of Assimilating Thermodynamic variables

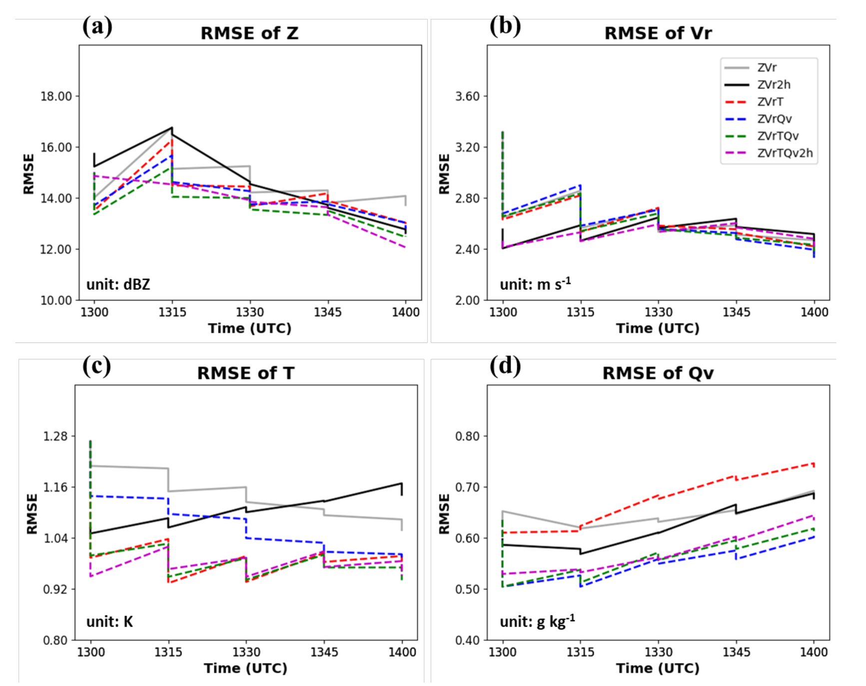

Fig. 4. Root mean square error in assimilation period.

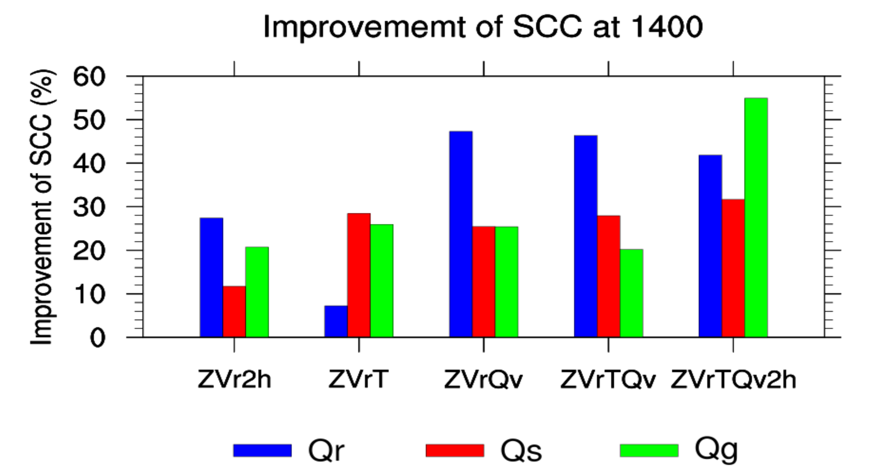

Fig. 5. Improvement of final ayalysis at 1400 UTC in spatial correlation coefficient of hydrometer variables compared with Exp. ZVr.

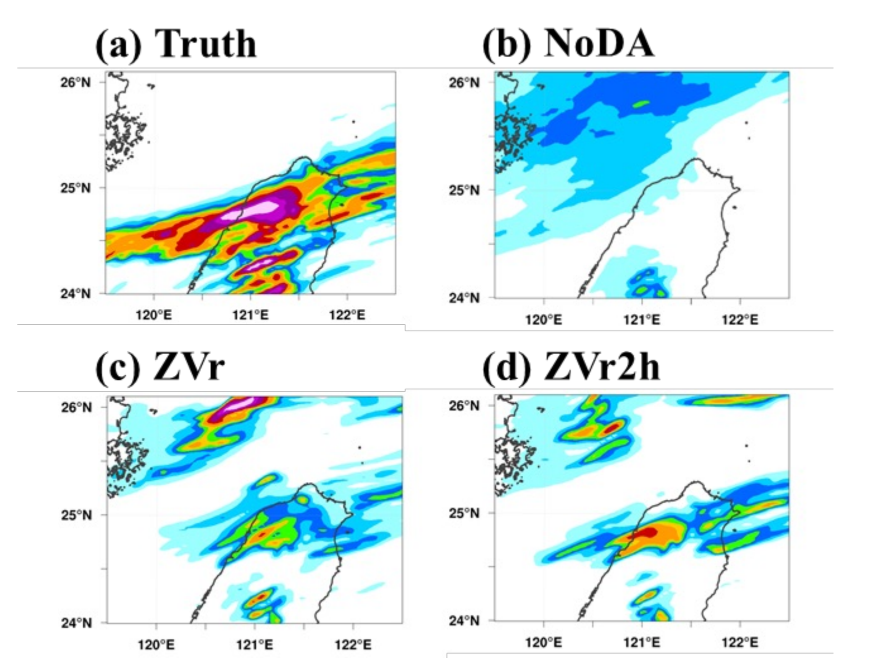

Fig. 6. Rainfall accumulation from 1400 UTC for 3-hrs

Analysis of assimilating retrieval variables

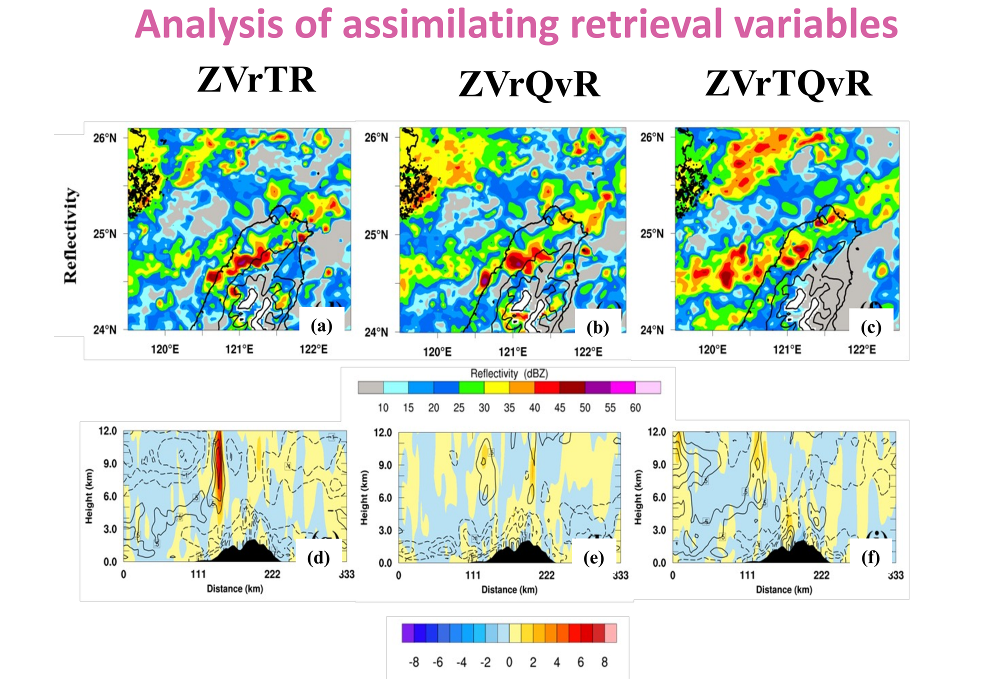

Fig. 7. Final analysis fields at 1400 UTC. Reflectivity field on 2.5-km height; Vertical velocity (shaded) and Potential temperature perturbation (contours)

Rainfall Forecast of assimilating retrieval variables

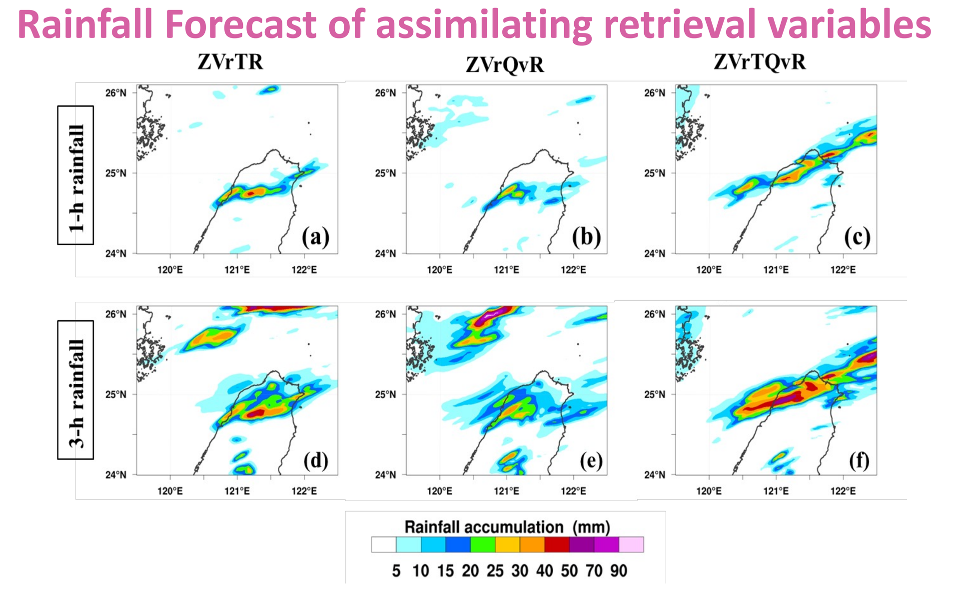

Fig. 8. Rainfall accumulation from 1400 UTC for 1-hr and 3-hrs

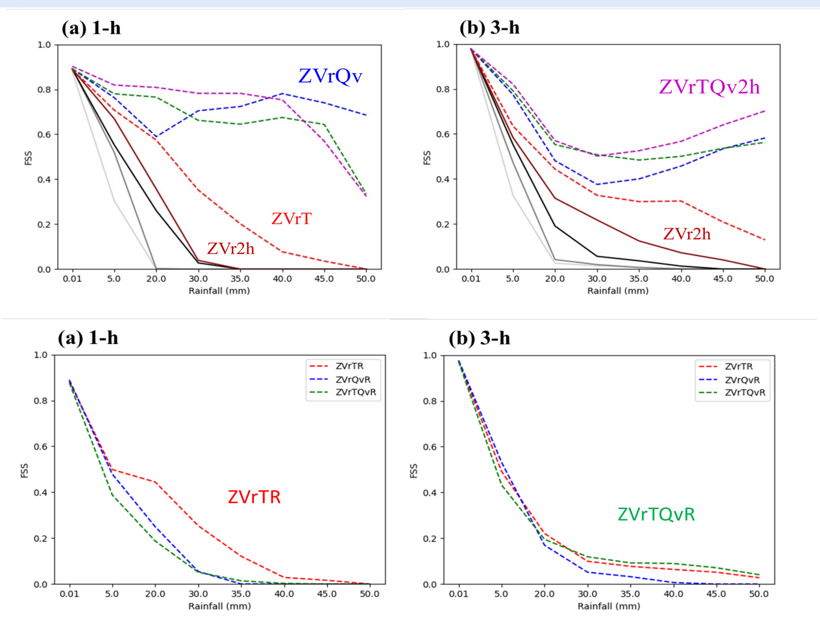

Fig. 9. Fractions Skill Score (FSS) for 1-hr and 3-hrs

SUMMARY

We discuss the feasibility of assimilating retrieval 3D thermodynamic with radar data. When the biased thermodynamic fields were obtained by a retrieval algorithm, assimilating temperature information reproduced a stronger upward motion and warm core at the convective area of the final analysis, and improved the very short-term QPF at the first hour.

T	*convection temperature and upward motion*	*Ice hydrometer*	*Very short-term QPF (1-h)*
Qv	*Wider cold pool*	*Warm hydrometer*	
T+Qv	*Stratiform temperature*		*QPF after 3-h → 6-h*

Future Works

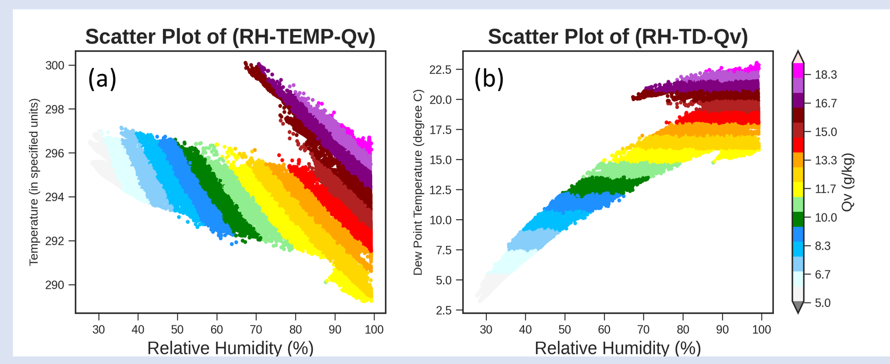

Fig. 10. The different type of temperature with relatively humidity, and water vapor mixing ratio.

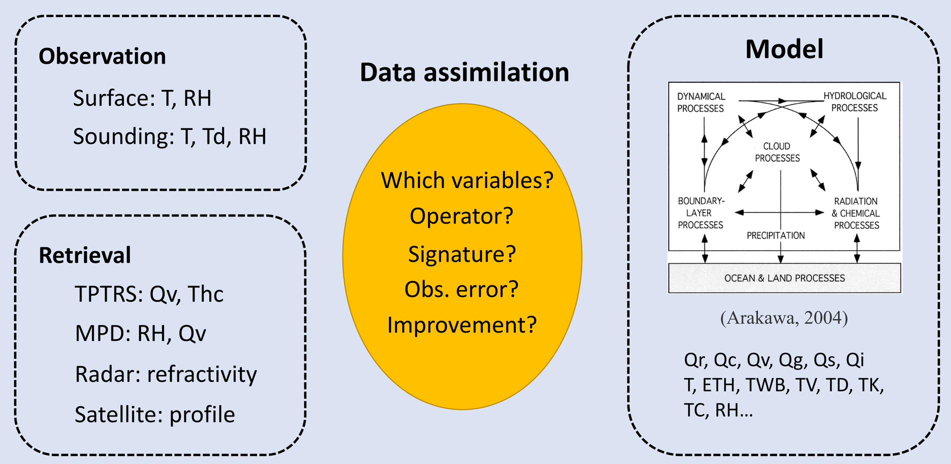

Acknowledgment

This work was supported by the Ministry of Science and Technology of Taiwan through Research Grant 108-2111-M-008-026, and NSTC 111-2811-M-008-073.

Reference

Ke, C.-Y., K.-S. Chung., Y.-C., Liou., C.-C. Tsai., 2022: Impact of Assimilating Radar Data With 3D Thermodynamic Fields in an Ensemble Kalman Filter: Proof of Concept and Feasibility. *Mon.Wea.Rev.*, **150**, 3251-3273.

Ke, C.-Y., K.-S. Chung, T.-C. Chen Wang, and Y.-C. Liou, 2019: Analysis of heavy rainfall and barrier-jet evolution during Mei-Yu season using multiple Doppler radar retrievals: a case study on 11 June 2012. *Tellus A: Dynamic Meteorology and Oceanography*, **71**, 1-21.

Liou, Y.-C., P.-C. Yang, and W.-Y. Wang, 2019: Thermodynamic recovery of the pressure and temperature fields over complex terrain using wind fields derived by multiple-Doppler radar synthesis. *Mon. Wea. Rev.*, **147**, 3843-3857.

Tsai, C.-C., S.-C. Yang, and Y.-C. Liou, 2014: Improving quantitative precipitation nowcasting with a local ensemble transform Kalman filter radar data assimilation system: observing system simulation experiments. *Tellus Series A-Dynamic Meteorology and Oceanography*, **66**, 1-18.